

16th Australasian Fluid Mechanics Conference
Crown Plaza, Gold Coast, Australia
2-7 December 2007

EXPERIMENTAL AND NUMERICAL STUDY OF A HYDROGEN FUELLED I.C. ENGINE FITTED WITH THE HYDROGEN ASSISTED JET IGNITION SYSTEM

A. A. Boretti, M. J. Brear, H. C. Watson

Department of Mechanical & Manufacturing Engineering, University of Melbourne, VIC, AUSTRALIA

Abstract

The use of hydrogen as an engine fuel poses several challenges as well as opportunities in engine design and control. These challenges are mainly due to hydrogen's high flame temperatures at near stoichiometric mixtures, as well as the reactant volume fraction which can reduce the engine power output significantly. However, the wide flammability limits of hydrogen combustion in air means that a large part of the engine operation regime can be achieved without the use of the engine throttle or exhaust after treatment. This paper presents results of experiments and computations for a research single cylinder pressure boosted hydrogen fuelled internal combustion engine (H₂ICE) fitted with the Hydrogen Assisted Jet Ignition system (HAJI) and running extremely lean mixtures.

Introduction

H₂ICE is a technology available today and economically viable in the near-term, with a number of test vehicles already presented [1-25]. This technology demonstrated efficiencies in excess of today's gasoline engines and operate relatively cleanly (NO_x is the only emission pollutant). There are fewer constraints concerning H₂ICE compared to fuel cells. A dual-fuel option (H₂/gasoline) is possible and fuel impurities are not an issue. Increased efficiencies, high power density and reduced emissions are possible in the future with multi-mode operating strategies and advancement in ICE design and materials.

Some properties of hydrogen, CNG and gasoline are presented in Table 1. The unique combustion properties of hydrogen can be beneficial at certain engine operating conditions and pose technical challenges at other engine operating conditions. Favourable properties of H₂ are the wide flammability range for ultra lean operation, the high laminar flame speed for good stability and the high octane number for high compression ratios with improved thermal efficiency. Unfavourable properties of H₂ are the high percentage stoichiometric volume fraction with the consequent air displacement effects, the low minimum ignition energy with consequent propensity to pre-ignite, and the small quenching distance for thin thermal boundary layers.

In port fuel injection (PFI) H₂ICEs, cold-start is not an issue because of the gaseous fuel, and NO_x is the only non-trivial engine-out emission pollutant (if we ignore the upstream emissions in producing hydrogen). To satisfy SULEV requirements, H₂ICEs must operate ultra-lean ($\lambda > 2.22$). However, there are a few fundamental and practical obstacles related to SULEV operating strategies in PFI-H₂ICEs. One of them is pre-ignition; the ignition of the fuel/air mixture before the spark plug fires. Ignition sources include residual gas causing back firing and engine hot spots, oil contaminants, and others [1]. These produce engine knock-like effects than can lead to engine damage. H₂ is predisposed to pre-ignition, and PFI H₂ICEs fuelled by compressed hydrogen gas are most susceptible. It is very difficult to operate PFI H₂ICEs at or near $\lambda = 1$ in practice and to avoid pre-ignition the engine is operated lean. Consequently, engine torque (and power) is significantly reduced. With stoichiometric operation and after treatment

practically inaccessible, continuous ultra-lean operation with no after treatment leads to low torque (power). Thus advanced H₂ICEs and SULEV operating strategies are needed.

Advanced H₂ICEs include pressure boosting (TC), liquid hydrogen fuelling, direct injection (DI), exhaust gas dilution (EGR) and multi-mode strategies. Pressure boosting allows continuous ultra-lean ($\lambda > 2.22$) operation with improved power densities. Accessible stoichiometric ($\lambda = 1$) operation with after treatment is obtained by using liquid hydrogen fuelling, exhaust gas dilution and direct injection. In liquid hydrogen fuelling, the cold mixture prevents pre-ignition and allows $\lambda = 1$ operation. With exhaust gas dilution operation, lean-burn conditions are diluted with EGR such that $\lambda = 1$ with no excess oxygen ($\lambda = 1.66$ operating point with 18% H₂, 44% air, 38% excess air is equivalent to a $\lambda = 1$ operating point with 18% H₂, 44% air, 38% EGR). With direct injection, the injection timing is optimized (delayed) to prevent pre-ignition and allow for $\lambda = 1$ operation. Direct injection may be used not only to produce a homogeneous H₂/air mixture, but also to create a stratified H₂/air mixture to reduce emissions and improve efficiency. The challenge is to deliver such a large fuel volume in a few crank angle degrees.

Table 1 - H₂ properties relevant to ICEs [12,13] (^a Liquid at 0 °C; ^b At stoichiometry; ^c Methane; ^d Vapor; ^e At 25 °C and 1 atm).

Property ^e	Hydrogen	CNG	Gasoline
Density (kg/m ³)	0.0824	0.72	730 ^a
Flammability limits (volume % in air)	4-75	4.3-15	1.4-7.6
Flammability limits (λ)	10-0.14	2.5-0.62	$\approx 1.43-0.25$
Auto ignition T in air (K)	858	723	550
Min. ignition energy (mJ) ^b	0.02	0.28	0.24
Flame velocity (m/s) ^b	1.85	0.38	0.37-0.43
Adiabatic flame T (K) ^b	2480	2214	2580
Quenching distance (mm) ^b	0.64	2.1 ^c	≈ 2
Stoichiometric fuel/air ratio	0.029	0.069	0.068
Stoichiometric vol. fraction	29.53	9.48	$\approx 2^d$
Lower heating value (MJ/kg)	119.7	45.8	44.79
Heat of combustion (MJ/kg air) ^b	3.37	2.9	2.83
Research octane number	> 120	140	91-99

A few multi-mode strategies are available. Operation may be ultra-lean ($\lambda > 2.22$) at low engine load, with exhaust gas dilution

(EGR) stoichiometric ($\lambda=1$) with after treatment at medium engine load and finally stoichiometric ($\lambda=1$) with after treatment at high engine load. Alternatively, it may be ultra-lean ($\lambda>2.22$) at low engine load and ultra-lean ($\lambda>2.22$) or lean ($\lambda\approx 1.43$) with lean NO_x trap (LNT) with pressure boosting supercharger at medium and high engine load. Or, in case of direct injection hydrogen fuelling, it may also be stratified ultra-lean ($\lambda>5$) at idle, ultra-lean ($\lambda>2.22$) at low engine load, stratified lean ($1<\lambda\leq 2.22$) with LNT after treatment at medium engine load, stratified stoichiometric ($\lambda=1$) with after treatment at high engine load.

This paper focuses on the development of a pressure boosted; throttle-less PFI- H_2 ICE. Combustion in the main chamber of a pressure boosted ASTM-CFR single cylinder research engine of homogeneous H_2 /air mixtures from stoichiometric to extremely lean is analysed experimentally and numerically. This engine is equipped with the Hydrogen Assisted Jet Ignition (HAJI) system.

The HAJI technology was developed and patented by the third author in 1992 to improve ignition of premixed mixtures of air and different fuels. High thermal efficiency may be achieved through reduced pumping, heat, and chemical dissociation losses and increased ratio of specific heats. In addition, the higher turbulent flame speed caused by the jets and chemically controlled active species produced by HAJI results in shorter burn duration of premixed mixtures of air and different fuels [2,3].

Single cylinder research engine

The test engine is an ASTM-CFR engine manufacturer by Waukesha Motor Co., Waukesha, Wisconsin, US. This is a single cylinder engine having capacity 611.7 cm^3 , bore 82.5 mm, stroke 114.3 mm, valve seat insert inside diameter 30.1 mm, connecting rod length 254.0 mm, ports minimum diameters 31.7 mm, compression ratio infinitely variable, combustion chamber plane cylindrical. Valve timings for the supercharged engine with valve clearance 0.25 mm are IVO= 15° BTDC, IVC= 50° ABDC, EVO= 50° BBDC, EVC= 15° ATDC. The standard engine is modified to accommodate the HAJI system on one side as described in Figure 1. For these particular tests, the HAJI orifice was inclined 15° upward and a groove was machined in the piston to reduce jet to piston interference running higher compression ratios.

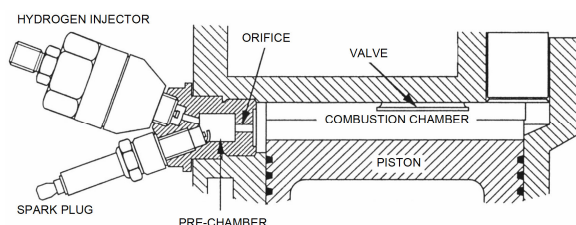


Figure 1 - Single cylinder CFR Engine with HAJI.

HAJI operates by injecting H_2 fuel consisting of 0.5 to 4% of the total fuel energy into a pre-chamber volume, which is as little as 0.7 to 1.5 % of the main chamber clearance volume. The process of combusting any main chamber fuel starts with the induction of air and fuel into the main chamber. After inlet valve closure, the main chamber mixture is compressed. Hydrogen is injected into the pre-chamber 90° BTDC and the injection duration lasts approximately 10° . After injection, the inflowing air-fuel mixture begins to mix with the H_2 inside the pre-chamber. Ignition is initiated by a small sparkplug which ignites the H_2 -air-fuel mixture. This ignition generates a turbulent jet. This jet then flows into the main chamber at high speeds, both mixing and

igniting the main chamber charge [2,3]. The HAJI nozzle used here has a single orifice of 2 mm diameter and 3 mm length and 0.9 cm^3 pre-chamber. The HAJI system uses a small 8 mm NGK spark plug, compared to the standard 18 mm spark plug. The overall size of the HAJI unit including pre-chamber and spark plug is designed such that it is possible to screw into the side of the block using an M18 thread, i.e. the standard spark plug hole. Consequently, when spark ignition is required, the HAJI unit is simply replaced with an 18 mm spark plug.

The pre-chamber contains a rich mixture, therefore combustion is incomplete and the jets are seeded with residual active species such as OH^\cdot and H^\cdot [2,3]. Using this system, the thermally and chemically active jet creates an ignition source, which consequently overcomes the problems associated with poorly mixed main chamber charges and the slow burn of fuels under extremely lean conditions.

Assuming speed has less effect on emissions than air-to-fuel ratio (AFR), a speed of 1800 rpm, corresponding to a typical engine speed when a vehicle is being tested over the NEDC cycle, is chosen for this study. Inlet temperature, port-induced cylinder motion, cam timing, and combustion chamber shape are held constant throughout the experiments and direct injection and external EGR are not explored. Eliminating these variables enable the target parameters such as CR, AFR, and MAP to be more thoroughly examined.

Experimental setup

A schematic layout of the experimental set up is presented in Figure 2. A Motec M4 engine control unit (ECU) is used to control spark timing and H_2 injector duration and timing. The ECU also allows for outputs to be logged in real-time via a computer interface. The use of a reference wheel and a GT101 Hall Effect sensor fitted to the camshaft allows the detection of both engine crank angle and cycle position. A Bosch ignition module (0227 100 124) is connected to a Bosch MEC 718 coil supplying energy to the spark plug with a transistorized coil ignition system. A Delco 3 bar MAP sensor allows the manifold air pressure to be monitored. In order to dampen fluctuations caused by pressure pulsations in the plenum, a small diameter copper tube restrictor is placed between the intake plenum and the MAP sensor. Establishing the reference for the spark timing is done with a timing light and later verified on a motoring curve. Considering peak cylinder pressure usually occurs at -0.5 - 1.5° BTDC, the accuracy of phasing is estimated to be within 0.5° .

In order to operate the CFR engine in boosted mode, a 200 litre tank pressurized to 8 bars is connected to the engine. Exhaust gas emissions are measured using an ADS 9000 Super Five Gas Analyser. It measures the concentrations of $\text{CO}(\%)$, $\text{CO}_2(\%)$, $\text{O}_2(\%)$, $\text{HC}(\text{ppm})$, and $\text{NO}_x(\text{ppm})$. These exhaust products are used to calculate the AFR by performing a chemical balance of the reactants and products. A Kistler 601B1 piezoelectric pressure transducer mounted in the cylinder head is connected to a 462-A-05 PCP charge amplifier and used for in-cylinder pressure measurement.

The main chamber H_2 flow is measured with a series of sonic nozzles calibrated for H_2 . The pre-chamber H_2 is measured by a digital Brooks 5860E gas flow meter. The air flow through the engine is measured with a calibrated orifice meter and the corresponding calibration constants were developed based on the British Standard BS1042.

Before any data is collected, the water jacket temperature circulating through the engine was consistently monitored and regulated to a steady value of 100°C . This also allowed the oil to warm up as the engine was run for approximately 15 minutes at $\lambda=1.6$ and 1800 rpm. This warm up period allowed the IMEP and

BMEP outputs to stabilize and the ADS9000 exhaust gas analyser to be warmed.

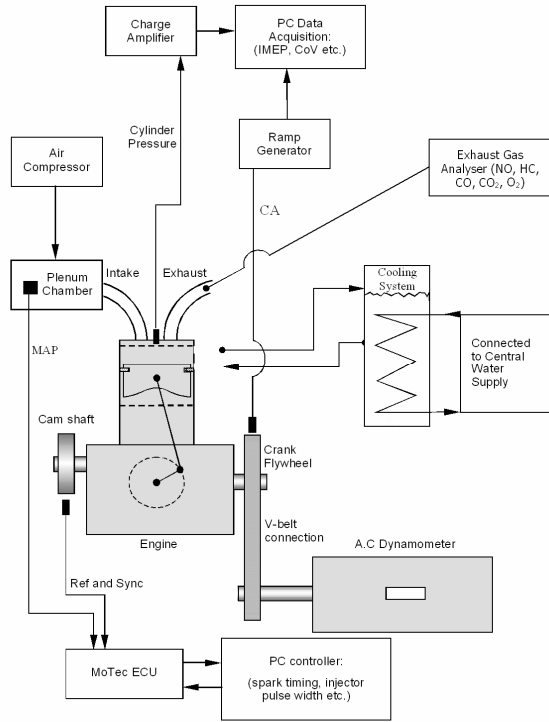


Figure 2 - Schematic layout of the engine including controllers, sensors and data acquisition systems.

CAE model

The operation of the ASTM–CFR single cylinder research engine with HAJI is also modelled by using the GT-POWER [26] CAE software. GT-POWER is an industry-standard engine simulation tool, specifically designed for both steady state and transient performance simulations, used by engine and vehicle makers and suppliers.

GT-POWER's 'predictive' SI turbulent flame combustion model is used in this paper. This model includes effects of the cylinder's geometry, spark-timing, charge motion and mixture properties. It is assumed that the combustion is flow driven once flame kernel becomes larger than the turbulent length scale. The initial growth of the flame depends on the laminar flame speed. This speed is a function of fuel, dilution, temperature and pressure. Once the flame grows larger, the speed is dominated by turbulence. This turbulent flame speed scales with the turbulence intensity.

The mass entrainment rate into the flame front and the burn rate are governed by the following equations:

$$\frac{dM_e}{dt} = \rho_u \cdot A_e \cdot (S_T + S_L)$$

$$\frac{dM_b}{dt} = \frac{(M_e + M_b)}{\tau}$$

$$\tau = \frac{\Lambda}{S_L}$$

where M_e is the entrained mass of the unburned mixture, t the time, ρ_u the unburned density, A_e the entrainment surface area at the edge of the flame front, S_T the turbulent flame speed, S_L the laminar flame speed, M_b the burned mass, τ the time constant, Λ

the Taylor micro scale length. The in-cylinder flow is described to provide a turbulence intensity and length scale.

We do not model the HAJI pre-chamber and we use an equivalent spark plug located at the exit of the HAJI jet to the main chamber. The geometry of the head and piston and the location of the equivalent spark plug define the geometry of the flame. Equivalent spark timing and initial spark size must be prescribed.

A laminar flame speed correlation is provided in [26] for H_2 down to an equivalence ratio of 0.1 below which flame quenches. This correlation is based on [27]. A correction is applied to the base flame speed to account for the effect of temperature, pressure and dilution. Once the flame entrains unburned mixture, the mixture is assumed to burn after a slight delay (based on flame thickness). The laminar flame speed is calculated by the following equation:

$$S_L = (B_m + B_\phi \cdot (\Phi - \Phi_m)^2) \cdot \left(\frac{T_u}{T_{ref}}\right)^\alpha \cdot \left(\frac{P}{P_{ref}}\right)^\beta \cdot (1 - 2.06 \cdot RMF^{0.77 \cdot \gamma})$$

where S_L is the laminar flame speed, B_m the maximum laminar speed, B_ϕ the laminar speed roll-off value, Φ the in-cylinder equivalence ratio, Φ_m the equivalence ratio at maximum speed, T_u the temperature of the unburned gas, RMF the mass fraction of the residuals in the unburned zone, α a temperature ratio exponent function of Φ [29], β a pressure ratio exponent function of Φ [29], γ a dilution exponent multiplier, T the temperature and P the pressure. The default constant laminar speed roll-off value B_ϕ is modified as a function of the intake flow equivalence ratio Φ_i to properly simulate combustion in extremely lean conditions with HAJI.

Results and discussion

In conventional spark plugs, the spark timing is the time of spark and the initial spark size is the same as the gap between the sparkplug electrodes. With HAJI, the spark plug ignites the richer pre-chamber mixture, and the jet then ignites the leaner main chamber mixture. For sake of simplicity, we take the equivalent spark timing equal to the HAJI spark timing, and we take the initial spark size as a standard 2 mm gap. However, for all simulations the flame kernel growth multiplier is then assumed to be a constant value larger than unity to simulate the faster first development of combustion with HAJI in this engine. The flame kernel growth multiplier influences the ignition delay, with larger numbers shortening the delay and advancing the transition from laminar combustion to turbulent combustion.

The turbulent flame speed multiplier is also used to scale the calculated turbulent flame speed. This variable influences the overall duration of combustion, with larger numbers increasing the speed of combustion. For all simulations, a constant value larger than unity is also used for this parameter to simulate the faster main combustion with HAJI in this engine.

Experiments and computations have been performed for the engine operating points (manifold air pressure MAP , equivalence ratio Φ , ratio of HAJI to total hydrogen, spark advance SA) presented in Table 2. Other engine operating conditions are engine speed 1800 rpm, compression ratio 11, HAJI injection timing 90° BTDC, water temperature 100° C and air pressure (dry) 99.5 kPa. Spark advances are not maximum brake torque (MBT) values. Experimental data was collected by Hamori in 2002 [3].

Results of experiments and computations are presented in Figure 3-6. Decreasing Φ has obvious effects: the air flow increases because the hydrogen flow reduces, the energy available for combustion reduces, the laminar flame speed reduces, the combustion rate deteriorates, the spark timing is advanced to compensate the reduced rate of combustion, the peak pressure reduces, *IMEP* reduces. As *MAP* increases, the air flow rate increases. However, *IMEP* does not increase proportionally to the air flow rate because of the different combustion rate and spark advance.

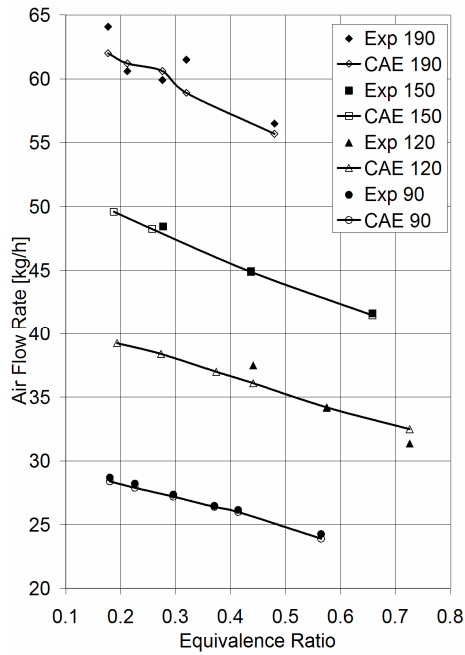


Figure 3 – Experimental and computational air flow rate vs. equivalence ratio.

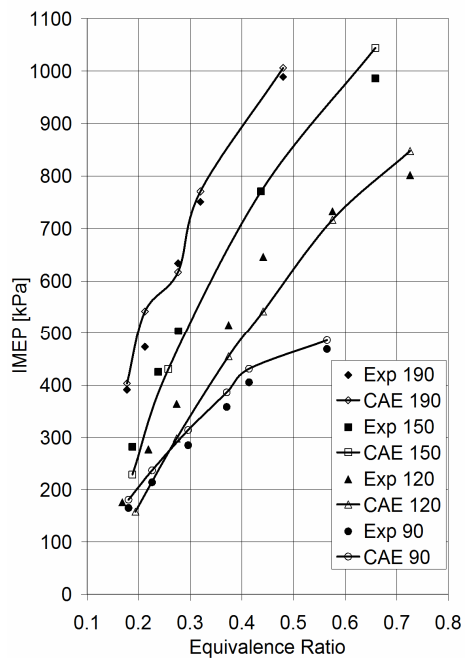


Figure 4 – Experimental and computational IMEP vs. equivalence ratio.

The presented experimental and computational results agree surprisingly well, and within the estimated accuracy of the numerical techniques and in spite of the unorthodox ignition system. When reference is made to standard spark plug ignition, these results show that HAJI can be modelled to an acceptable degree for design purposes at least in a reasonably orthodox manner. Of course, HAJI increases the flame speed, and produces a faster growth rate of the flame kernel, for an advanced transition from laminar combustion to turbulent combustion, and a faster main turbulent combustion.

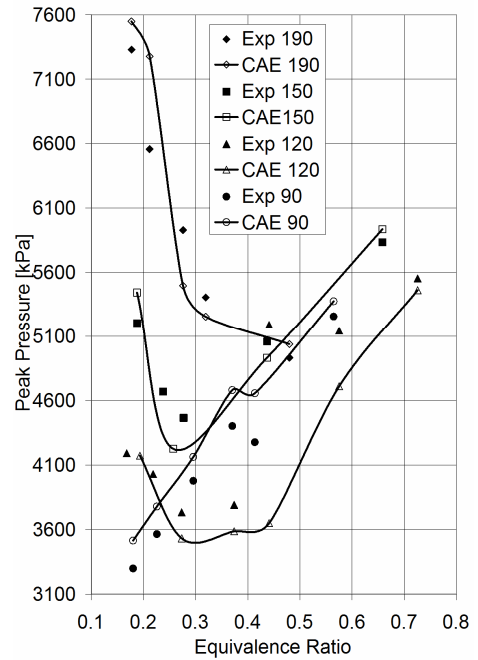


Figure 5– Experimental and computational peak pressure vs. equivalence ratio.

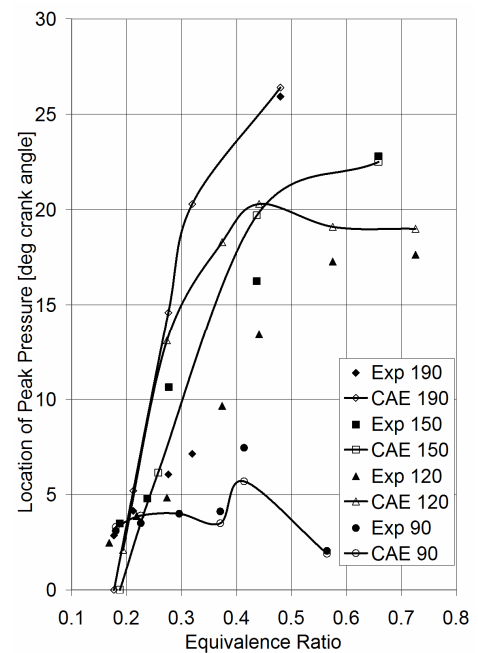


Figure 6 – Experimental and computational location of peak pressure vs. equivalence ratio.

Table 2 – Engine operating points.

MAP [kPa]	Φ Tot.	HAIJ/Tot.H ₂	SA [deg]
90	0.564	0.024	20
90	0.413	0.031	22
90	0.370	0.034	28
90	0.295	0.041	32
90	0.226	0.053	36
90	0.180	0.065	40
120	0.734	0.146	-1
120	0.581	0.169	2
120	0.446	0.200	5
120	0.378	0.255	7
120	0.277	0.342	14
120	0.221	0.414	26
120	0.170	0.519	48
150	0.666	0.121	-3
150	0.442	0.169	5
150	0.280	0.247	9
150	0.240	0.296	15
150	0.190	0.375	36
190	0.486	0.122	-1
190	0.323	0.169	5
190	0.279	0.200	15
190	0.214	0.258	27
190	0.179	0.292	45

The spark ignition turbulent combustion model parameters have to be recalibrated with experiments for different engine configurations to adjust the effects of turbulence intensity and length scale.

Conclusions

This paper has presented results of experiments and computations for a hydrogen fuelled internal combustion engine (H₂ICE) fitted with the Hydrogen Assisted Jet Ignition (HAJI) system. The engine used pressure boosting and continuous operation to ultra-lean over a range of equivalence ratios and manifold air pressures. The measured influence of equivalence ratio, manifold air pressure and spark advance is captured surprisingly well by the simulations. Of course, experiments and computations then also agree very well for air flow and *IMEP* values.

This study shows that simple and computationally inexpensive SI turbulent flame combustion models may be used for engine design if experimental data for the particular application are collected first. Validation of the model is an essential element of its application. When reference is made to standard spark plug ignition, these results show that HAJI can be modelled in a reasonably orthodox manner. HAJI is observed to increase the flame speed and produces a faster growth rate of the flame kernel, for an earlier transition from laminar combustion to turbulent combustion, and a faster main turbulent combustion.

Acknowledgements

The authors wish to thank Mr. J. Cromas and Mr. S. Wahiduzzaman of Gamma Technologies Inc., Westmont, IL for their suggestions on combustion modelling, and E. Toulson and W. Attard for assistance in preparing this manuscript. This work was supported by the Advanced Centre for Automotive Research and Testing (ACART).

References

- [1] Watson, H.C., E.E. Milkins, W.R.B. Martin, and J. Edsell, "An Australian hydrogen car", Department of Mechanical and Industrial Engineering, University of Melbourne, 1983.
- [2] Hamori, F. and Watson, H. C., "Hydrogen Assisted Jet Ignition for the Hydrogen Fuelled SI Engine", paper presented at the "World Hydrogen Energy Conference No. 15", Lyon, FR, May 2006.
- [3] Hamori, F., "Optimising the application of HAJI to the supercharged engine", University of Melbourne PhD Thesis, Parkville, Melbourne, AU, 2006.
- [4] Danner, S., Fuerst, S., "BMW hydrogen 7 series – a safe way to a clean future", Paper presented at the Fisita 2006 World Congress, Yokohama, JP, Oct. 2006. F2006M088.
- [5] Berger, E., Bock, C., Fischer, H., Gruber, M., Kiesgen, G., Rottengruber, H., "The new BMW 12-cylinder hydrogen engine as clean efficient and powerful vehicle power train", Paper presented at the Fisita 2006 World Congress, Yokohama, JP, Oct. 2006. F2006P114.
- [6] Verhelst S., Verstraeten S., Sierens R., "Combustion strategies and NO_x emissions for hydrogen fuelled IC engines", Paper presented at the Fisita 2006 World Congress, Yokohama, JP, Oct. 2006. F2006P092.
- [7] Saito T., Matsushita M., Mitsugi H., Ueda T., "Development of hydrogen rotary engine with dual-fuel system", Paper presented at the Fisita 2006 World Congress, Yokohama, JP, Oct. 2006. F2006P200.
- [8] Mohammadi, A., Shioji, M., Nakai, Y., Ishikura, W., Tabo, E., "Injection strategy for a direct-injection SI hydrogen engine", Paper presented at the Fisita 2006 World Congress, Yokohama, JP, Oct. 2006. F2006P368.
- [9] Bosma, H., Buning, L., Dalhuijsen, W., Merts, M., "Gaseous fuels containing hydrogen in internal combustion engines", Paper presented at the Fisita 2006 World Congress, Yokohama, JP, Oct. 2006. F2006P412.
- [10] J. Yamin, "Comparative study using hydrogen and gasoline as fuels: Combustion duration effect", Int. J. Energy Res., vol. 30 (2006), pp. 1175–1187.
- [11] Mohammadi, A., Shio, M., Naka, Y., Ishikura, W., Tabo, E., "Performance and combustion characteristics of a direct injection SI hydrogen engine", International Journal of Hydrogen Energy, vol. 32 (2007), pp. 296 – 304.
- [12] C. White, "A Technical Review of Hydrogen-Fuelled Internal Combustion Engines", paper presented to the California Air Resources Board ZEV Technology Symposium, Cal/EPA Headquarters, Sacramento, CA, Sep. 2006.
- [13] C.M. White C.M., Steeper, R.R., Lutz, A.E., "The hydrogen-fuelled internal combustion engine: a technical review", International Journal of Hydrogen Energy, vol. 31 (2006), pp. 1292 – 1305.
- [14] Li, H., Karim, G.A., "Knock in spark ignition hydrogen engines", International Journal of Hydrogen Energy, vol. 29 (2004), pp. 859– 865.
- [15] Heffel, J.W., "NO_x emission and performance data for a hydrogen fuelled internal combustion engine at 1500 rpm using exhaust gas recirculation", International Journal of Hydrogen Energy, vol. 28 (2003), pp. 901–908.
- [16] Heffel, J.W., "NO_x emission reduction in a hydrogen fuelled internal combustion engine at 3000 rpm using exhaust gas

- recirculation”, *International Journal of Hydrogen Energy*, vol. 28 (2003), pp. 1285–1292.
- [17] Lee, J. T., Kim, Y. Y., Lee, C. W., Caton, J.A., “An Investigation of a Cause of Backfire and Its Control Due to Crevice Volumes in a Hydrogen Fuelled Engine”, *Journal of Engineering for Gas Turbines and Power*, Jan. 2001, Vol. 123, pp. 204-210.
- [18] Sisiopiku, V.P., Rousseau, A., Fouad, F.H. and Peters, R.W., “Technology Evaluation of Hydrogen Light-Duty Vehicles”, *Journal of Environmental Engineering*, Jun. 2006, pp.568-574.
- [19] Li, H., and Karim, G.A., “Hydrogen Fuelled Spark-Ignition Engines Predictive and Experimental Performance”, *Journal of Engineering for Gas Turbines and Power*, Jan. 2006, Vol. 128, pp. 230-236.
- [20] Li, H., Kim, Y.Y., and Caton, J.A., “The Development of a Dual-Injection Hydrogen-Fuelled Engine With High Power and High Efficiency”, *Journal of Engineering for Gas Turbines and Power*, Jan.2006, Vol. 128 , pp. 203-212.
- [21] Attar, A.A., and Karim, G.A., “Knock Rating of Gaseous Fuels”, *Journal of Engineering for Gas Turbines and Power*, Apr. 2003, Vol. 125, pp.500- 504.
- [22] Kim, Y.Y, Lee, J.T., and Caton, J.A., “The Development of a Dual-Injection Hydrogen-Fuelled Engine with High Power and High Efficiency”, *Journal of Engineering for Gas Turbines and Power*, Jan. 2006, Vol. 128, pp. 203-212.
- [23] Sierens, R., and Verhelst, S., “Influence of the Injection Parameters on the Efficiency and Power Output of a Hydrogen Fuelled Engine”, *Journal of Engineering for Gas Turbines and Power*, Apr. 2003, Vol. 125, pp.444-449.
- [24] Sierens, R., and Verhelst, S., “Experimental Study of a Hydrogen-Fuelled Engine”, *Journal of Engineering for Gas Turbines and Power*, Jan. 2001, Vol. 123, pp.211- 216.
- [25] G. D’Errico, A. Onorati, S. Ellgas, A. Obieglo, “Thermo-fluid dynamic simulation of a S.I. single-cylinder h2 engine and comparison with experimental data”, *Proceedings of ICES2006 ASME Internal Combustion Engine Division 2006 Spring Technical Conference, Aachen, GE, may 2006*.
- [26] http://gtisoft.com/broch_gtpower.html
- [27] M. O Conaire, H.J. Curran, J.H.Simmie, W.J.Pitz, C.H. Westbrook, “A Comprehensive Modelling Study of Hydrogen Oxidation”, *International journal of chemical kinetics*, vol. 36 (11), pp. 603-622, Nov. 2004.
- [28] T. Morel, S. Wahiduzzaman, S. Sheard, “Comparison of Measured and Predicted Combustion Characteristics of a Four Valve S.I. Engine”, SAE P. 930613.
- [29] J. B. Heywood, *Internal Combustion Engine Fundamentals*, McGraw Hill, New York, US, 1988.